# THERMAL CONSEQUENCES OF LAND USE DYNAMICS IN THE PADMA BRIDGE ECONOMIC CORRIDOR: A REMOTE SENSING PERSPECTIVE

**Md Shariful Islam Shuvo*[1], Md Nahidul Islam[2], Nusrat Jahan[3] and Md Mahmudun Nabi[4]**

[1] *Department of Civil Engineering, Gopalganj Science and Technology University, Gopalganj-8105, Bangladesh, e-mail: shariful.islam.shuvo25@gmail.com*
[2] *Department of Civil Engineering, Gopalganj Science and Technology University, Gopalganj-8105, Bangladesh, e-mail: mni.nahid.24@gmail.com*
[3] *Department of Civil Engineering, Gopalganj Science and Technology University, Gopalganj-8105, Bangladesh, e-mail: nusrathjahanpromi210@gmail.com*
[4] *Lecturer, Gopalganj Science and Technology University, Gopalganj-8105, Bangladesh, e-mail: shohan.ce098@gmail.com*

***Corresponding Author**

## ABSTRACT

The rapid transformation of land use and land cover (LULC) in emerging economic corridors introduces significant thermal stress on local environments, posing challenges for sustainable urban planning. In the context of the Padma Bridge Economic Corridor specifically the unions near the Padma Bridge in Zajira upazila along with Shibchar, Srinagar and Louhajang upazilas, where intensified infrastructural activities such as road expansion, industrialization and institutional proposals are accelerating. Land Surface Temperature (LST) serves as a crucial indicator of these changes, reflecting the thermal response of the surface to altered land cover and human induced modifications. This study focuses on quantifying the thermal consequences of LULC dynamics using remote sensing. Unlike cities in northwestern Bangladesh such as Rajshahi which already exhibit chronic heat issues, this corridor is now experiencing new, infrastructure driven thermal dynamics due to recent land cover changes. Focusing on four primary LULC classes vegetation, built-up area, waterbody and bare soil, Landsat images from 2004, 2014 and 2024 were classified using maximum likelihood supervised classification method with ArcGIS and the classification accuracy was evaluated through the kappa accuracy assessment using Google Earth Pro. Land Surface Temperature (LST) was derived using radiative transfer and mono-window algorithms, integrating NDVI based emissivity correction. In order to ascertain how changes in land use affected surface thermal properties over time, the link between LULC change and LST variation was evaluated during the study years (2004, 2014 and 2024) using statistical analysis and spatial comparison in ArcGIS. In the Padma Bridge Economic Corridor, built-up areas expanded from 9.21% to 20.46% among 2004 and 2024, vegetation decreased from 42.11% to 36.48% and bare land stabilized at about 25%. The total transition matched a steady rise in temperature, even while water bodies shown a partial recovery that may have been impacted by hydrological alteration and natural processes including erosion, sedimentation. There was a noticeable thermal increase throughout the corridor, with the mean temperature of land surface rising from 20.87°C to 22.94°C and the percentage of places above 24°C growing from less than 2% in 2004 to almost 18% by 2024. These trends represent a developing microclimatic shift caused by fast infrastructural growth, indicating the onset of an urban heat environment along the Padma Bridge Economic Corridor.

***Keywords:*** *LULC, LST Analysis, Sustainable Urban Development, Padma Bridge, Remote Sensing*

## 1. INTRODUCTION

Land cover modification driven by intensified anthropogenic activities is a widespread phenomenon globally, with particularly high rates observed in developing countries such as Bangladesh (Abdullah et al., 2022). Numerous studies have examined the factors contributing to rapid land use and land cover (LULC) change, identifying population growth (El-Zeiny & Effat, 2017; Yohannes et al., 2021), economic affluence, industrialization, and rural-to-urban migration (Abdullah et al., 2022) as significant drivers. The rapidly rising urban population drastically affects the natural distribution of land use and it creates negative impacts on urban land surface temperature(LST) (Argüeso et al., 2014; Bahi et al., 2016; Un-Habitat, 2016). The continuous urban growth around the Padma Bridge project highlights the need to closely examine its effects on land use changes and land surface temperature. Bangladesh's social and economic development has been significantly influenced by the Padma Bridge (Khan, 2022), especially in surrounding areas like Zajira, Shibchar, Srinagar and Louhajang upazilas. The regions which surround the bridge's approach and connector zones have seen a sharp increase in land development, infrastructure and urban-rural ties. The bridge has improved transport efficiency, industrial growth and investment opportunities, making these unions vital components of the Padma Bridge Economic Corridor. As transport, settlements and industries grow, land use and land cover (LULC) are changing noticeably. These changes impact the local environment and increase land surface temperature (LST), causing shifts in the local climate(Salan & Bhuiyan, 2024). Around the world, satellite remote sensing (RS) and Geographic Information System (GIS) are widely used for creating maps and studying spatial information (Al Rakib et al., 2020). In Bangladesh, many studies have examined LULC changes and their effects on LST over the years in cities such as Dhaka, Rajshahi, Chittagong and Khulna(Ahmed, 2011b, 2011a; Al Kafy et al., 2020; Hussain et al., 2016; Yamane et al., 2014). Comprehensive studies linking LULC and LST are still limited for the Padma Bridge's surrounding upazilas, namely Zajira, Shibchar, Srinagar and Louhajang. These upazilas have experienced rapid urban growth, especially over the past decade and many researchers suggest that this expansion has contributed to a significant rise in temperature in the area.

The purpose of that study is to classify and produce changing map in ecological cover and land use across selected years (for 2004, 2014 and 2024) in Zajira, Shibchar, Srinagar and Louhajang upazilas, to derive and analyse thermal consequences of land use to examine the spatial corelation among LULC dynamics and LST variations and to identify emerging thermal hotspots and environmentally vulnerable zones within the study area. However, this study provides essential data for environmental management and planning in the Padma Bridge–influenced areas. The results can help guide sustainable development policies and heat-mitigation strategies in Zajira, Shibchar, Srinagar and Louhajang upazilas.

## 2. MATERIALS AND METHODS

### 2.1 Description of Study Area

This study covers the upazilas around the Padma Bridge within Zajira Upazila (Shariatpur District), Shibchar Upazila (Madaripur District), Sreenagar and Louhajang Upazilas (Munshiganj District) as shown in Table 1. This corridor centers on the Padma Multipurpose Bridge which is Bangladesh's longest road-rail bridge opened in 2022 to link the southwest directly with Dhaka.

Louhajang Upazila in Munshiganj District is located at the eastern end of the Padma Bridge near Mawa. Along the bridge, fresh houses, markets and businesses are appearing, contributing to the area's rapid growth. To the northeast, Sreenagar Upazila has both farmland and homestead areas which are slowly changing as better roads and urban growth reach the region. On the western side of the Padma Bridge, Zajira Upazila in Shariatpur District serves as the bridge's western end where rural areas and riverside villages are gradually turning into urban and industrial zones. Figure 1 illustrates the spatial visualization of the study area prepared using ArcGIS.

Table 1: Area & Coordinate of Upazilas along Padma Bridge

| Upazila | District | Area (km²) | Latitude (Approx.) | Longitude (Approx.) |
|---|---|---|---|---|
| Zajira | Shariatpur | 246.21 | 23.35° N | 90.33° E |
| Shibchar | Madaripur | 332.90 | 23.25° N | 90.16° E |
| Sreenagar | Munshiganj | 203.00 | 23.53° N | 90.29° E |
| Louhajang | Munshiganj | 131.10 | 23.47° N | 90.35° E |

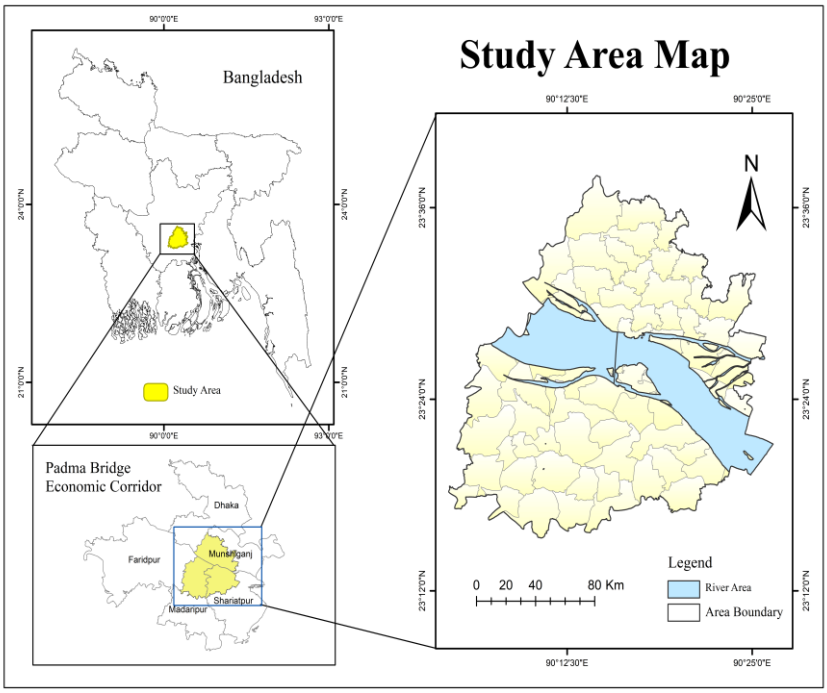


Figure 1: Study Area

Next to it, Shibchar Upazila in Madaripur District contains key sections of the Dhaka-Bhanga Expressway, as well as new interchanges and industrial sectors which are transforming the region's land use and landscape. The climate of this region is nearly similar to that of Dhaka. The summer months March to June are usually hot and humid with temperatures often exceeding 35°C. In July to October, the monsoon season brings significant rainfall and high humidity whereas the winter months November to February are cooler and dry. In recent years, increasing urban development around the bridge area has contributed to increased regional heating and visible changes in surface temperature patterns.

## 2.2 Data Description

This study utilizes multi-temporal Landsat satellite images along with meteorological data. Several satellite images from Landsat of 2004, 2014 and 2024 is obtained by the official website of United States Geological Survey as detailed in Table 2. To reduce temporal change in the thermal environment investigation, three data sets from Landsat satellites were gathered, throughout the similar period. To keep from cloud coverage, the coverage of clouds had been reduced to under 10% nonetheless scene cloud cover was nearly 0% in all datasets. The level of spatial accuracy of all the data was 30 metres.

Table 2: Specifications of the Essential Satellite Imagery

| Satellite | Year | Sensor | Acquisition Date | Land Cloud Cover | Path/Row | Resolution |
|---|---|---|---|---|---|---|
| Landsat 5 | 2004 | Thematic Mapper (TM) | 29 November 2004 | 0.00 | 137/44 | 30 m |
| Landsat 8 | 2014 | Operational Land Imager (OLI) | 25 November 2014 | 0.01 | | |
| | 2024 | | 20 November 2024 | 0.12 | | |

### 2.3 Identification of Land Use and Land Cover

Water bodies, built-up areas, vegetation areas and bare land are the four categories into which the LULC is split as summarized in Table 3. From satellite image, firstly all the bands are composited. Then Image modification, optimization and transformation are all done during the initial processing stages. Image classification is the automatic analysis of remotely sensed images and the majority of image classification relies only on the identification of the spectral fingerprints of land cover classes (Lillesand & Kiefer, 1994). Geometric correction is used to eliminates geometric errors. After removing atmospheric influences, the objective of atmospheric correction is to restore surface reflection, which is a representation of surface attributes, from remotely taken photos. It has been found that the atmospheric correction greatly improves the accuracy of image classification (Bue et al., 2015). During pre-processing and preparation, the most commonly applied maximum likelihood supervised classification (MLSC) technique was used to map all LULC classes. Before the training sample was carried out, a rigorous examination of the research area's Google Earth photos, field trips, and satellite imagery was done. In order to enhance classification accuracy, a minimum of 100 training samples have been acquired for each land cover category. Total accuracy, Kappa coefficient and accuracy validation were used to evaluate the accuracy of land use classification.

Table 3: Overview of LULC Classes

| LULC Classes | Description |
|---|---|
| Built-Up Area | Residential, industrial and commercial |
| Vegetation | Trees, fallow land and grassland |
| Water Body | River, reservoirs, wetlands and lakes |
| Bare Land | Char land, bare soils and landfill places |

### 2.4 Constructing a Map of LST

Surface temperature of the land is closely linked to the LULC pattern. Surface temperature will be measured for this study use the USGS satellite's thermal bands picture data in 2004, 2014 and 2024. A three and seven-step method were followed for Landsat 4-5 TM and Landsat 8 OLI images respectively.

### 2.5 LST estimation for Landsat 4-5 TM images

The Landsat 5 Thematic Mapper's band 6 (10. 40μm - 12. 50μm) is used to estimate LST and for Landsat 8 Land Imager band 10 TIRS 1 (10.6μm - 11.19μm) and band 11 TIRS 2 (11.5μm - 12. 51μm) are used to estimate LST. Firstly, the values of the Digital Number (DN) of the temperature zones are transformed to sensor radiance using the following equation (1), equation (2) (Faridatul, 2017).
For Landsat 6,

$$Radiance\ L_\lambda = \left(\frac{L_{max\lambda} - L_{min\lambda}}{QCal_{max} - QCal_{min}}\right) * (QCal - QCal_{min}) + L_{min\lambda} \quad (1)$$

Where,
$L_{\max\lambda}$ = Max. Radiance of Band 6 $L_{\min\lambda}$ = Min. Radiance of Band 6,
$QCal$= Quantized Calibrated Pixel value, $QCal_{max}$ = Max. quantized calibrated pixel value
$QCal_{min}$ = Min. quantized calibrated pixel value

For Landsat 8,

$$Radiance\ L_\lambda = M_L * QCal + A_L \quad (2)$$

Where, $M_L$ = radiance multiplicative scaling factor; $A_L$ = Band's radiation exponential scaling factor;
$QCal$ = Pixel value

Secondly, the thermal band calibration constants ( $K_1$ & $K_2$) are obtained from the metadata files of the corresponding years and the satellite temperature, T (in degree Celsius) is calculated using Equation (3)

$$T = \frac{K_2}{ln\left(\frac{K_1}{L_\lambda}\right)} - 273.15 \quad (3)$$

where, $K_1$ & $K_2$ = Thermal Band Calibration Constants
Lastly, the land surface temperature is estimated using Equation (4)

$$LST = \frac{T}{1+\left(\frac{\lambda T}{\rho}\right)*ln(\varepsilon)} \quad (4)$$

where,
$\lambda$ = Central band wavelength, $T$= Satellite temperature, $\varepsilon$= Emissivity, $\rho = 438\times10^{-2}$ mK
Emissivity is determined by following equation (5)

$$Emmissivity(\varepsilon) = 0.004P_v + 0.986 \quad (5)$$

where,
$P_v$= index of plants (determined by executing the algorithm) using equation (6)

$$P_v = \left[\frac{NDVI - NDVI_{min}}{NDVI_{max} - NDVI_{min}}\right]^2 \quad (6)$$

## 3. RESULTS AND DISCUSSIONS

### 3.1 Land Use Land Cover

The classified maps for 2004, 2014 and 2024 (Figure 2) shows four major land cover types: water bodies, vegetation, built-up areas and bare land. Their changes over two decades clearly indicate the transformation accomplished by regional development and the Padma Multipurpose Bridge Project.

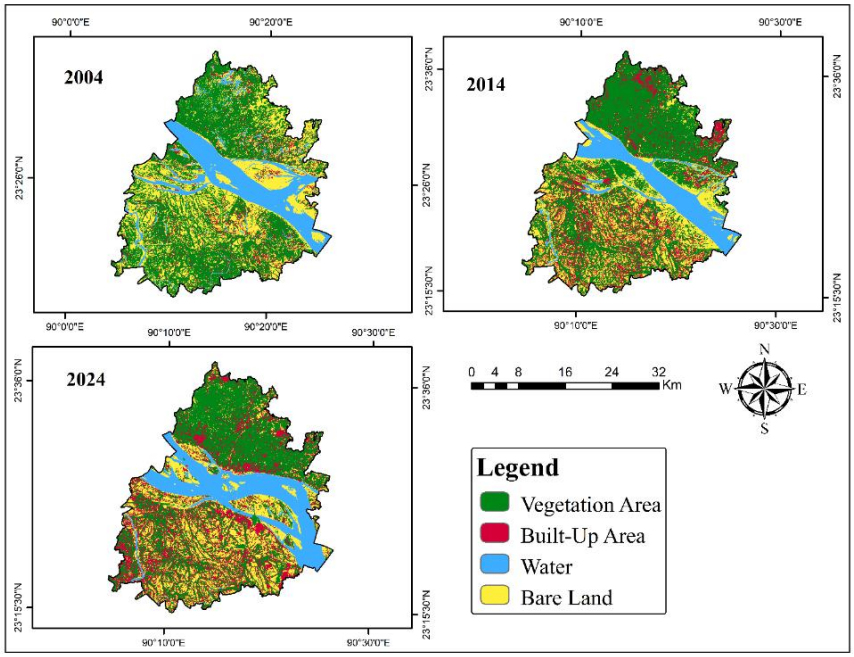


Figure 2: Land Use Land Cover Map

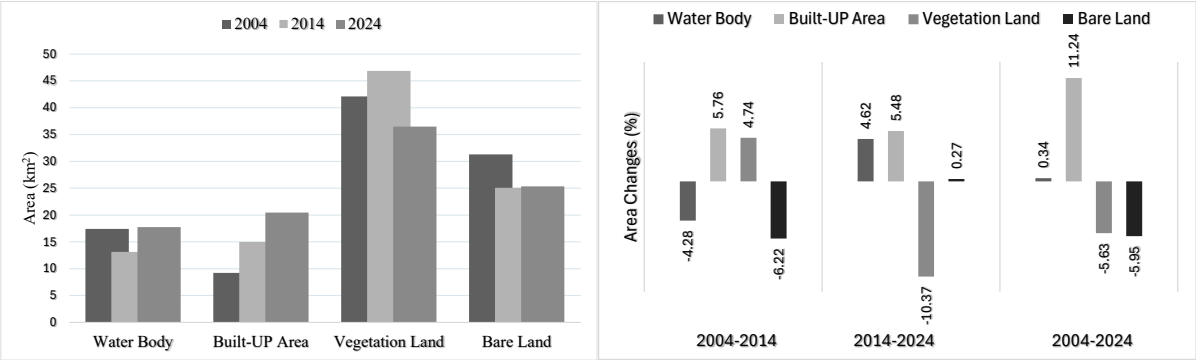


Figure 3: Distribution of LULC (Left), Gains and Losses of the Land Cover (Right)

Table 4: Distribution of LULC

| Individual Year | Area | | | | | | Change (%) | | |
|---|---|---|---|---|---|---|---|---|---|
| | 2004 | | 2014 | | 2024 | | 2004-2014 | 2014-2024 | 2004-2024 |
| LULC Classes | km² | % | km² | % | km² | % | | | |
| Water Body | 164.45 | 17.40 | 124.03 | 13.13 | 167.65 | 17.74 | -4.28 | 4.62 | 0.34 |
| Built-Up Area | 87.07 | 9.21 | 141.52 | 14.98 | 193.30 | 20.46 | 5.76 | 5.48 | 11.24 |
| Vegetation Land | 397.86 | 42.11 | 442.60 | 46.84 | 344.66 | 36.48 | 4.74 | -10.37 | -5.63 |
| Bare Land | 295.52 | 31.28 | 236.75 | 25.06 | 239.29 | 25.32 | -6.22 | 0.27 | -5.95 |

In 2004, vegetation land dominated the area, covering about 42.11% (397.86 km²), with bare land at coming in second at 31.28% (295.52 km²) as detailed in Table 4. Only 9.21% (87.07 km²) was made up of built-up land, whereas 17.40% (164.45 km²) were occupied by water bodies. Figure 3 illustrates the 2014 map showing a slow but noticeable increase in vegetation to 46.84% (442.60 km²) and built-up land to 141.52 km² (14.98%), which is probably due to partial regeneration and pre-construction landscaping in some areas. However, as new infrastructure and populations arose around the bridge route, the built-up area increased dramatically to 193.30 km² (20.46%) by 2024. While bare ground stayed mostly constant at roughly 25%, vegetation decreased to 36.48% (344.66 km²), a slight decrease from previous years. Water bodies had a minor recovery from 13.13% in 2014 to 17.74% in 2024, perhaps as a result of channel rehabilitation and excavation during development. The spatial patterns demonstrate a harmony between environmental change and growth. While changes in vegetation and bare ground represent cycles of land clearance and stabilization, the resulting increase in built-up areas indicates fast urban growth following the bridge's construction.

### 3.2 Assessment of Classified LULC Map Accuracy

Ground-truth samples and error matrices were used to evaluate the classification correctness of all three Landsat-derived LULC maps. In 2004, 2014 and 2024, the corresponding Kappa coefficient values were 0.87, 0.91 and 0.8. When the coefficient of Kappa exceeds 0.75, the degree of accuracy can be defined as extremely good (Foody, 2002; Pontius & Millones, 2011; Story & Congalton, 1986). The applied supervised sorting strategy produced dependable discrimination among land-cover groups, as evidenced by the consistently high overall classification accuracy (90.41% in 2004, 92.91% in 2014, and 91.25% in 2024) (Table 5). Mixed pixel effects along the riverbed may cause some differences in accuracy between years. However, the obtained accuracy levels are sufficient for long-term spatiotemporal analysis, guaranteeing that the results of LST extraction and subsequent change detection are grounded in reliable land-cover representation.

Table 5: Accuracy Assessment

| Classified Map | Kappa Index | Overall Accuracy |
|---|---|---|
| 2004 | 0.87 | 90.41% |
| 2014 | 0.91 | 92.91% |
| 2024 | 0.88 | 91.25% |

### 3.3 Changes in LULC

The temporal comparison of classified maps (Figure 5) and corresponding area statistics shows distinct land transformation trends over the 20-year duration. Between 2004 and 2014, Built-up area grew by 5.76% (54.45 km²) while vegetation gained 4.74% (44.74 km²). These changes coincided with gradual rural development prior to major bridge construction. In contrast, water bodies and bare land decreased by 4.28% and 6.22% respectively, possibly due to reclamation of floodplains and natural sediment deposition along the Padma River.

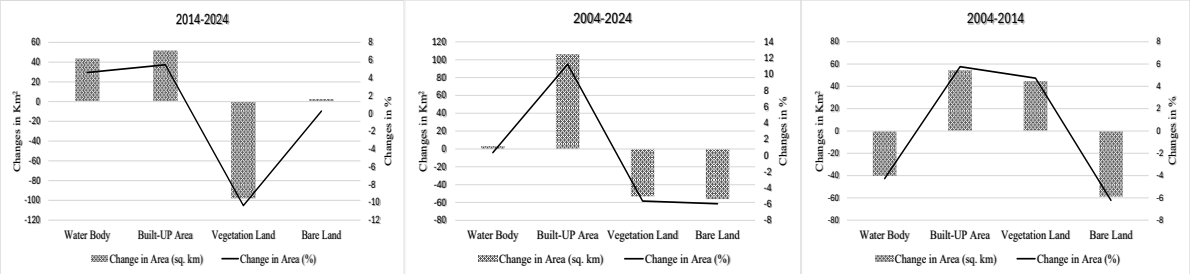


Figure 4: LULC Changes Over Period

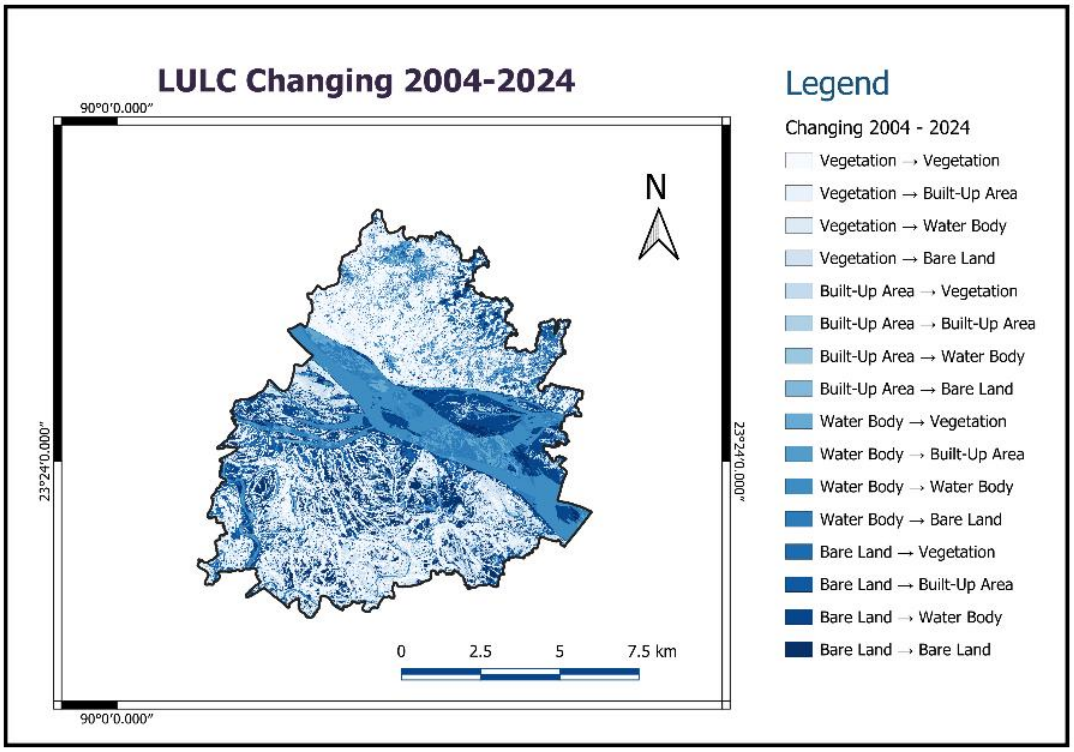


Figure 5: Transition of LULC over 2004-2024

The following ten years (2014–2024) show a significant change in land use trends as depicted in Figure 4. Since 2004, built-up land has increased by an additional 5.48%, for a total growth of 11.24%. This shift is in line with the construction of new transportation, commercial and residential networks that serve the bridge corridor. Infrastructure and cities have replaced agricultural and green spaces, as seen by the dramatic 10.37% (97.94 $km^2$) decrease in vegetation. Water bodies grew somewhat (4.62%), probably as a result of local embankment projects and hydrological restoration, whereas bare land stayed almost unchanged with a tiny increase of 0.27%. Overall, vegetation decreased by more than 5% while built-up land almost doubled between 2004 and 2024. These modifications highlight the quick rate of land conversion associated with the Padma Bridge's socioeconomic development. The region's surface temperature, runoff characteristics, and biological balance are all directly impacted by the redistribution of land use.

### 3.4 Variations in Land Surface Temperature

A gradual increase in thermal intensity is shown throughout the study area according to acquired land surface temperature (LST) maps for 2004, 2014, and 2024 (Figure 6). From below 18 °C to above 30 °C, the LST values were divided into eight groups (Table 6). The majority of the region (about 61.6%) was in the 20-22 °C range in 2004, with very little coverage at higher temperatures. Nearly half of the region had temperatures between 20 and 22 °C by 2014, while 20.6% achieved temperatures between 22 and 24 ° C. With more than 52% of the surface registering between 22 and 24 °C and almost 18.5% between 24 and 26 °C in 2024, a distinct warming trend became apparent. A tiny but noteworthy portion even rose above 28 °C, something that had not happened in previous years.

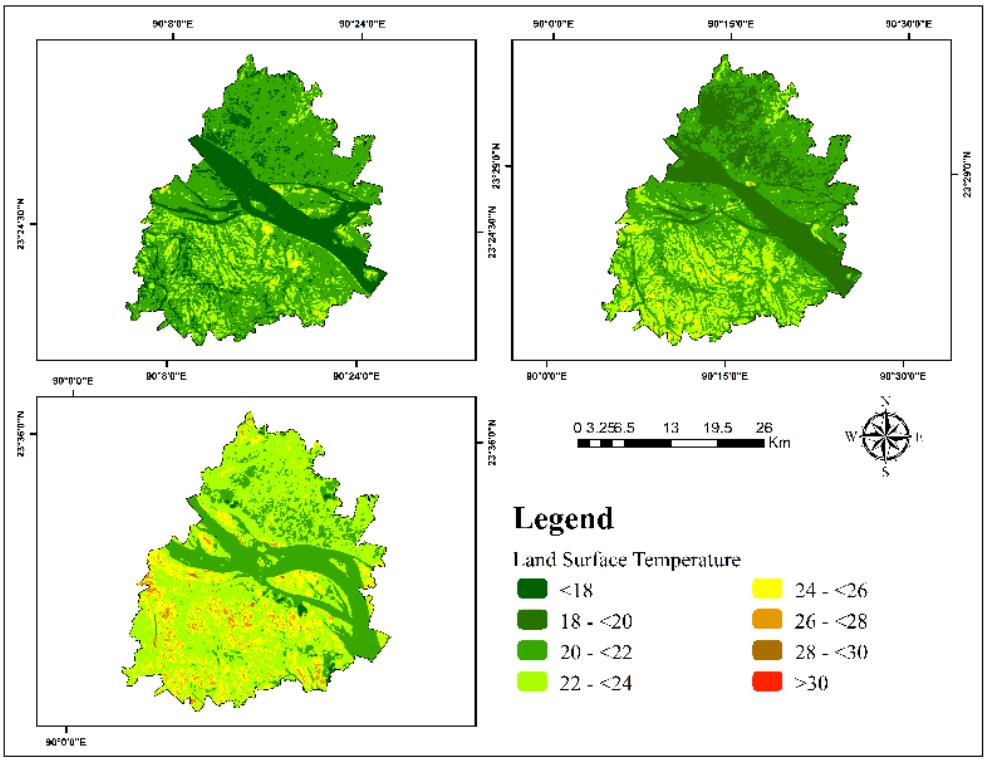


Figure 6: Land Surface Temperature 2004, 2014, 2024

This observation is strengthened by the thermal statistics summary (Table 6). From 20.87°C in 2004 to 21.03°C in 2014 and 22.94°C in 2024, the mean LST increased gradually. Over the course of two decades, the maximum temperature ever recorded rose from 27.18°C to 31.21°C. As heterogeneous surfaces including concrete, soil and plant interacted under changing land-use conditions, the standard deviation also significantly increased, indicating increased thermal variability throughout the landscape.

Table 6: Distribution of LST

| Ranges of LST (◦c) | 2004 | | 2014 | | 2024 | |
|---|---|---|---|---|---|---|
| | km$^2$ | % | km$^2$ | % | km$^2$ | % |
| <18 | - | - | .001 | 0.00 | 3.44 | 0.36 |
| 18 - <20 | 217.87 | 23.06 | 242.81 | 25.70 | 2.58 | 0.27 |
| 20 - <22 | 582.27 | 61.63 | 476.07 | 50.39 | 239.22 | 25.32 |
| 22 - <24 | 134.47 | 14.23 | 194.58 | 20.59 | 499.26 | 52.84 |
| 24 - <26 | 9.98 | 1.06 | 30.82 | 3.26 | 174.37 | 18.46 |
| 26 - <28 | 0.25 | 0.03 | 0.55 | 0.06 | 24.37 | 2.58 |
| 28 - <30 | - | - | - | - | 1.52 | 0.16 |
| >30 | - | - | - | - | 0.06 | 0.01 |
| Total | 944.84 | 100.00 | 944.83 | 100.00 | 944.82 | 100.00 |

The combined effects of changing land cover and growing impermeable surfaces are shown in this gradual warming (Figure 7). By decreasing evapotranspiration and increasing heat absorption, the post-bridge development has enhanced surface heating. While flora and bodies of water serve as cooling factors, bare soil and populated areas typically absorb more heat throughout the day and slowly release it at night.

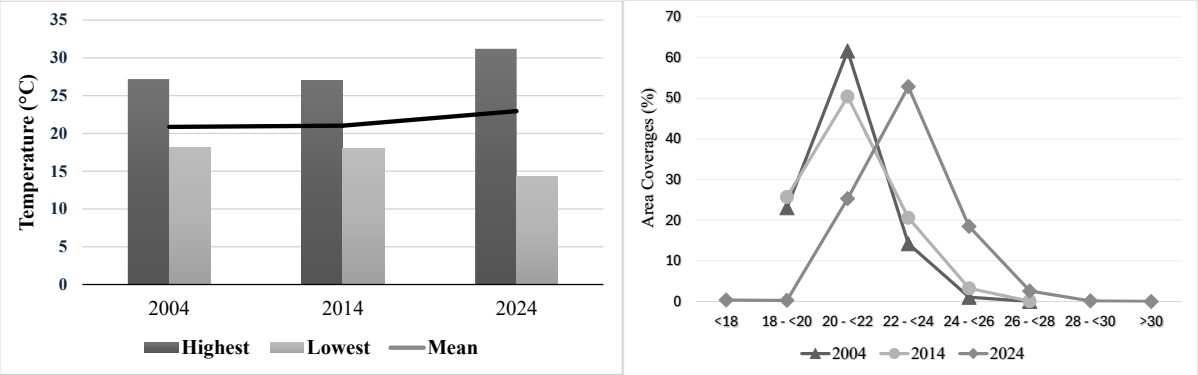


Figure 7: LST Summaries (Left), Distribution of LST (Right)

### 3.5 Validation of Estimated LST

Temperature records from the Bangladesh Agricultural Research Council (BARC) for 2004 and 2014 were used (Table 7) to validate LST computed from Landsat thermal bands; however, no field data were available for 2024. Since there is no BARC station in the study area and our Landsat images were taken at the end of November, which reflects the early winter conditions of December, the November and December temperature data from the two closest stations, Dhaka and Faridpur, were averaged to represent the local climate. There was only a slight difference between the recorded and estimated values. The highest and lowest calculated LST in 2004 were 27.18 °C and 18.18 °C, respectively, with variations of +0.95 °C and –1.05 °C from the BARC values of 28.13 °C and 17.13 °C. The corresponding variances in 2014 were –1.31 °C and +0.43 °C. The estimated LST closely matches ground-based measurements and may be trusted for additional spatial analysis and interpretation since the average deviation stayed below the standard deviation values (1.15–1.46 °C) derived from ArcGIS analysis.

Table 7: Validation of LST with Respect to BARC Documented Data

| Year | 2004 | | 2014 | | 2024 | |
|---|---|---|---|---|---|---|
| Source of Estimated/Recorded LST | Highest | Lowest | Highest | Lowest | Highest | Lowest |
| LST Estimated from Thermal Bands (˚C) | 27.18 | 18.18 | 27.04 | 17.98 | 31.21 | 14.56 |
| BARC Recorded Temperature (˚C) | 28.13 | 17.13 | 27.47 | 16.67 | - | - |
| Deviation | -0.95 | 1.05 | -0.43 | 1.31 | - | - |
| Average Deviation | 1 | | 0.87 | | - | |
| Standard Deviation from Thermal Bands | 1.15 | | 1.42 | | 1.46 | |
| Mean LST (˚C) | 20.87 | | 21.03 | | 22.94 | |

### 3.6 LULC vs LST Profiles

Using Pearson's correlation approach, a correlation analysis among LST and the main land surface classifications was carried out in SPSS. The findings showed a substantial negative correlation (r = -0.86) between vegetation and LST and a strong positive correlation (r = 0.89) between built-up area and LST. These numbers imply that while vegetation clearly has a cooling effect, urban growth increases surface heating. However, these associations were not statistically significant because of the small number of temporal samples, which reduces the relationship's strength. The correlation's robustness is limited by the tiny dataset, necessitating additional study using bigger sample sizes or temporal data with higher resolution. So, the impact of land-use dynamics on surface temperature throughout the study area was visually and quantitatively verified by additional spatial analysis of LST distribution in ArcGIS, which strengthened the interpretation.

Table 8: LST Distribution over Different Land Cover

| Year | LULC Class | LST(°C) | | | Std. Deviation |
|---|---|---|---|---|---|
| | | Minimum | Maximum | Mean | |
| 2004 | Vegetation Land | 19.06 | 24.25 | 20.41 | 0.69 |
| | Built-Up | 20.07 | 25.83 | 21.16 | 0.68 |
| | Water | 18.18 | 22.25 | 19.14 | 0.51 |
| | Bare Land | 21.06 | 27.18 | 22.77 | 1.11 |
| 2014 | Vegetation Land | 18.25 | 26.18 | 20.76 | 0.91 |
| | Built-Up | 18.18 | 26.73 | 21.8 | 1.38 |
| | Water | 17.98 | 21.8 | 19.22 | 0.25 |
| | Bare Land | 18.45 | 27.04 | 22.13 | 1.44 |
| 2024 | Vegetation Land | 16.63 | 27.07 | 22.65 | 0.75 |
| | Built-Up | 17.29 | 30.01 | 23.32 | 1.62 |
| | Water | 14.56 | 24.99 | 21.3 | 0.43 |
| | Bare Land | 18.9 | 31.21 | 24.37 | 1.29 |

The average LST values for various classes in 2004 varied from 22.77 °C in bare land to 19.14 °C in aquatic bodies shown in Table 8. The intermediate means for vegetation and built-up regions were 20.41°C and 21.16°C, respectively. These variations are consistent with the predicted warming effect of exposed soil and the cooling effect of plants. The temperature difference between classes somewhat increased by 2014. While vegetation and water stayed colder at 20.76 °C and 19.22 °C, built-up areas attained an average of 21.80 °C and bare land 22.13 °C. The most noticeable difference is seen in the 2024 scenario, where the mean temperature was 23.32 °C in built-up areas and 24.37 °C in bare land, while it was 22.65 °C in vegetation and 21.30 °C in water bodies. There was localized heating in exposed and construction-dominated areas, as evidenced by the maximum temperature of 31.21 °C within bare land. The direct impact of land cover type on surface thermal behaviour is confirmed by these changes. Elevated LST is the result of more solar energy being absorbed and retained by built-up and bare surfaces. Conversely, aquatic and vegetation areas promote evaporative cooling, which lowers LST. The spatial comparison shows that new thermal hotspots developed around the bridge approach roads and nearby urban expansion zones as vegetation and open water areas decreased.

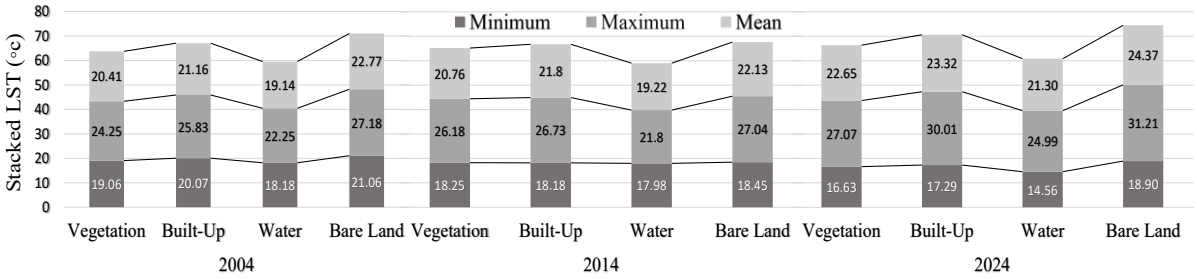


Figure 8: LST over LULC

As illustrated in Figure 8, the trend between 2004 and 2024 demonstrates the substantial regional correlation between changes in temperature and land use dynamics. The rise in impermeable surfaces is strongly correlated with the average temperature increase of roughly 2 °C over the course of two decades. This trend reflects the beginning of an urban heat island effect, in which the local microclimate is changed by development-driven heating.

## 4. CONCLUSIONS

Over the past two decades, the Padma Bridge Economic Corridor has undergone substantial LST associated with the Padma Multipurpose Bridge project, with ~ 2,693 ha of land were acquired between 2006 and project completion for the 6.15 km bridge and associated infrastructure, with major construction carried out between 2014 and 2022.

This study identifies three key outcomes concerning land use change and surface temperature dynamics:

1. Built-up areas expanded from 9.21% to 20.46%, while vegetation cover declined by more than 5%, coinciding with an increase in mean LST from 20.87°C to 22.94°C over the same period.
2. Bare or char lands consistently exhibited the highest surface temperatures, with maximum LST values exceeding 28 °C in 2024, indicating strong association with localized thermal hotspots.
3. Water bodies showed partial spatial recovery between 2014 and 2024 and consistently maintained lower LST values compared to others; however, their spatial extent and distribution remain influenced by erosion and sedimentation processes.

Taken together, expanding built-up areas and elevated LST indicates the early emergence of an urban heat island like condition along the Padma Bridge corridor. Although the satellite data were acquired in late November under early winter conditions, warming trend reflects a persistent microclimatic shift rather than seasonal variability alone. These findings highlight the importance of incorporating heat sensitive land use planning, preservation of vegetation cover and protection of surface water systems to support environmentally sustainable development within the Padma Bridge Economic Corridor.

## ACKNOWLEDGEMENTS

The authors gratefully acknowledge the Bangladesh Bridge Authority, from whose Padma Multipurpose Bridge Project online portal information on the Padma Bridge was obtained. Appreciation is also extended to the Bangladesh Agricultural Research Council (BARC) for providing surface temperature data and to the United States Geological Survey (USGS) for granting access to the Landsat archives.

## DECLARATION

During the preparation of this work the author's used Quilbot, Grammarly in order to improve language and readability, with caution. After using the tool/service, the author's reviewed and edited the content as needed and takes full responsibility for the content of the publication.

## REFERENCES

Abdullah, S., Barua, D., Abdullah, Sk. Md. A., & Rabby, Y. W. (2022). Investigating the Impact of Land Use/Land Cover Change on Present and Future Land Surface Temperature (LST) of Chittagong, Bangladesh. Earth Systems and Environment, 6(1), 221–235.

Ahmed, B. (2011a). Modelling spatio-temporal urban land cover growth dynamics using remote sensing and GIS techniques: A case study of Khulna City. Journal of Bangladesh Institute of Planners, 15–32.

Ahmed, B. (2011b). Urban land cover change detection analysis and modeling spatio-temporal Growth dynamics using Remote Sensing and GIS Techniques: A case study of Dhaka, Bangladesh. Universidade NOVA de Lisboa (Portugal).

Al Kafy, A., Al-Faisal, A., Mahmudul Hasan, M., Sikdar, Md. S., Hasan Khan, M. H., Rahman, M., & Islam, R. (2020). Impact of LULC Changes on LST in Rajshahi District of Bangladesh: A Remote Sensing Approach. Journal of Geographical Studies, 3(1), 11–23.

Al Rakib, A., Akter, K. S., Rahman, M. N., Arpi, S., & Kafy, A.-A. (2020). Analyzing the pattern of land use land cover change and its impact on land surface temperature: A remote sensing approach in Mymensingh, Bangladesh. Student Res.

Argüeso, D., Evans, J. P., Fita, L., & Bormann, K. J. (2014). Temperature response to future urbanization and climate change. Climate Dynamics, 42(7–8), 2183–2199.

Bahi, H., Rhinane, H., Bensalmia, A., Fehrenbach, U., & Scherer, D. (2016). Effects of urbanization and seasonal cycle on the surface urban heat island patterns in the coastal growing cities: A case study of Casablanca, Morocco. Remote Sensing, 8(10), 829.

Bue, B. D., Thompson, D. R., Eastwood, M., Green, R. O., Gao, B.-C., Keymeulen, D., Sarture, C. M., Mazer, A. S., & Luong, H. H. (2015). Real-time atmospheric correction of AVIRIS-NG imagery. IEEE Transactions on Geoscience and Remote Sensing, 53(12), 6419–6428.

El-Zeiny, A. M., & Effat, H. A. (2017). Environmental monitoring of spatiotemporal change in land use/land cover and its impact on land surface temperature in El-Fayoum governorate, Egypt. Remote Sensing Applications: Society and Environment, 8, 266–277.

Faridatul, M. I. (2017). Spatiotemporal effects of land use and river morphological change on the microclimate of Rajshahi metropolitan area. Journal of Geographic Information System, 9(4), 466–481.

Foody, G. M. (2002). Status of land cover classification accuracy assessment. Remote Sensing of Environment, 80(1), 185–201.

Hussain, M., Alak, P., & Azmz, I. (2016). Spatio-temporal analysis of land use and land cover changes in Chittagong city corporation, Bangladesh. Int. J. Adv. Remote Sens. GIS Geogr, 4, 56–72.

Khan, M. F. A. (2022). Exploring Hazard Risks and People's Adjustment: A Study in the Downstream of the Padma Multipurpose Bridge Project

Lillesand, T. M., & Kiefer, R. W. (1994). Remote sensing and image interpretation.

Pontius, R. G., & Millones, M. (2011). Death to Kappa: Birth of quantity disagreement and allocation disagreement for accuracy assessment. International Journal of Remote Sensing, 32(15), 4407–4429.

Salan, M. S. A., & Bhuiyan, M. A. H. (2024). Estimating impacts of micro-scale land use/land cover change on urban thermal comfort zone in Rajshahi, Bangladesh: A GIS and remote sensing based approach. Urban Climate, 58, 102187.

Story, M., & Congalton, R. G. (1986). Accuracy assessment: A user's perspective. Photogrammetric Engineering and Remote Sensing, 52(3), 397–399.

Un-Habitat. (2016). World cities report 2016: Urbanization and development-Emerging futures. UN.

Yamane, Y., Kiguchi, M., Terao, T., Murata, F., & Hayashi, T. (2014). Climatic Variability. In A. Dewan & R. Corner (Eds), Dhaka Megacity (pp. 61–73). Springer Netherlands.

Yohannes, H., Soromessa, T., Argaw, M., & Dewan, A. (2021). Impact of landscape pattern changes on hydrological ecosystem services in the Beressa watershed of the Blue Nile Basin in Ethiopia. Science of the Total Environment, 793, 148559.